AD-A099 494 ARMY ARMAMENT RESEARCH AND DEVELOPMENT COMMAND ABERD--ETC F/G 20/6
DETERMINATION OF OPTICAL CONSTANTS FROM EXTINCTION MEASUREMENTS--ETC(U)
APR 81 M E MILHAM, R H FRICKEL, J F EMBURY

UNCLASSIFIED ARCSL-TR-81031 SBIE-AD-E410 396 NL

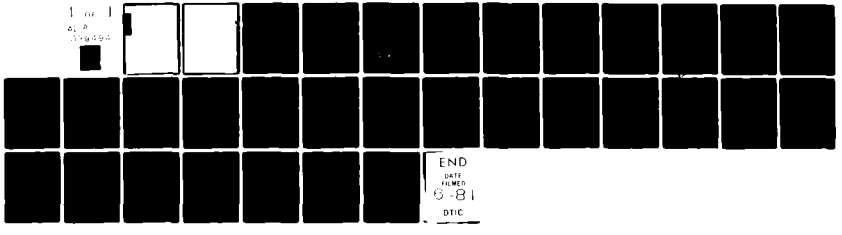

END
DATE FILMED
6-81
DTIC

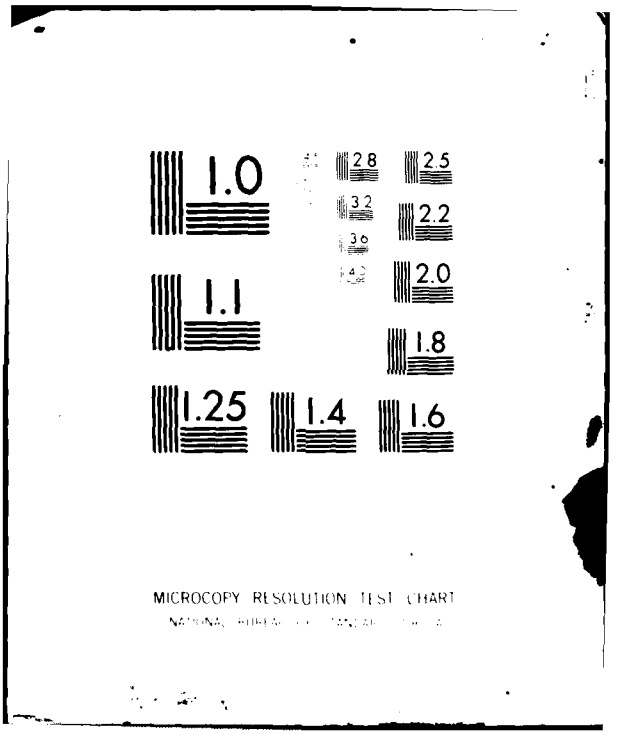
1.0
2.8
2.5
3.2
2.2
3.6
2.0
1.1
1.8
1.25
1.4
1.6
MICROCOPY RESOLUTION TEST CHART

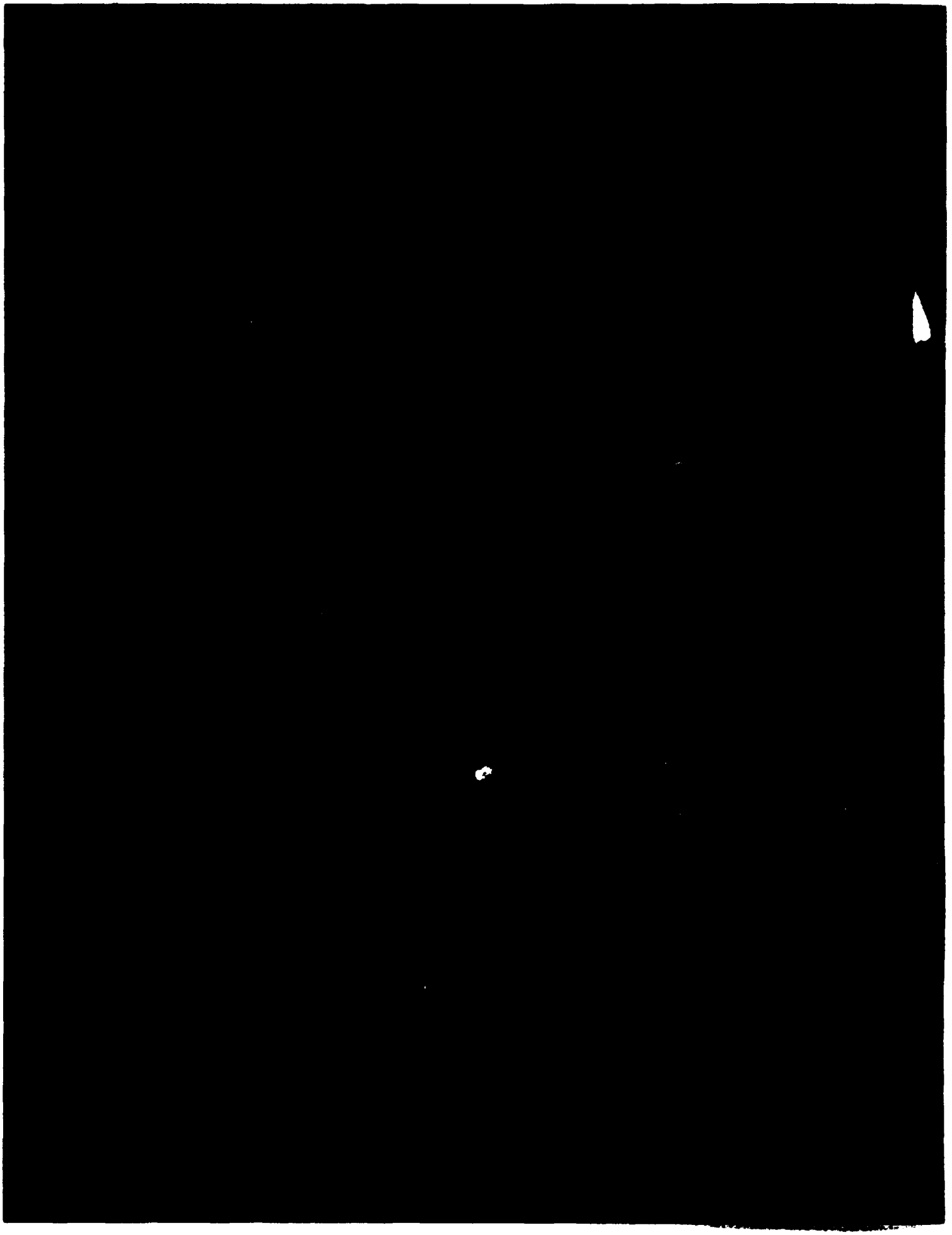

UNCLASSIFIED

SECURITY CLASSIFICATION OF THIS PAGE (When Data Entered)

REPORT DOCUMENTATION PAGE	READ INSTRUCTIONS BEFORE COMPLETING FORM
1. REPORT NUMBER: ARCSL-TR-81031	2. GOVT ACCESSION NO.: AD-A099 494 / 3. RECIPIENT'S CATALOG NUMBER
4. TITLE (and Subtitle): DETERMINATION OF OPTICAL CONSTANTS FROM EXTINCTION MEASUREMENTS	5. TYPE OF REPORT & PERIOD COVERED: Technical Report April–September 1980
	6. PERFORMING ORG. REPORT NUMBER
7. AUTHOR(s): M. E. Milham, J. F. Embury, R. H. Frickel, D. H. Anderson	8. CONTRACT OR GRANT NUMBER(s)
9. PERFORMING ORGANIZATION NAME AND ADDRESS: Commander/Director, Chemical Systems Laboratory, ATTN: DRDAR-CLB-PS, Aberdeen Proving Ground, Maryland 21010	10. PROGRAM ELEMENT, PROJECT, TASK AREA & WORK UNIT NUMBERS: Project 1L162662A554
11. CONTROLLING OFFICE NAME AND ADDRESS: Commander/Director, Chemical Systems Laboratory, ATTN: DRDAR-CLJ-R, Aberdeen Proving Ground, Maryland 21010	12. REPORT DATE: April 1981
	13. NUMBER OF PAGES: 33
14. MONITORING AGENCY NAME & ADDRESS(if different from Controlling Office)	15. SECURITY CLASS. (of this report): UNCLASSIFIED
	15a. DECLASSIFICATION/DOWNGRADING SCHEDULE: NA

16. DISTRIBUTION STATEMENT (of this Report)

Approved for public release; distribution unlimited.

17. DISTRIBUTION STATEMENT (of the abstract entered in Block 20, if different from Report)

18. SUPPLEMENTARY NOTES

19. KEY WORDS (Continue on reverse side if necessary and identify by block number)

Optical constants
Particulate materials
Aerosols
Extinction data
o-Phosphoric acid
Kramers-Kronig analysis
Lorenz-Mie calculations

20. ABSTRACT (Continue on reverse side if necessary and identify by block number)

Traditional methods of determining the optical constants of particulate materials by means of transmission, absorption, and reflectance measurements are known to be inherently inaccurate. The use of the Lorenz-Mie formalism to derive the optical constants from extinction data overcomes the problems associated with the traditional methods; but, as currently practiced, this method has severe limitations. In this paper, we report an entirely new approach to determining the optical

(Continued on reverse side)

DD FORM 1 JAN 73 1473 EDITION OF 1 NOV 65 IS OBSOLETE

UNCLASSIFIED

SECURITY CLASSIFICATION OF THIS PAGE (When Data Entered)

20. ABSTRACT (Contd)

constants of aerosols from extinction data. This is an iterative method which uses the Lorenz-Mie formalism in conjunction with the Kramers-Kronig dispersion relations in order to derive the optical constants of the aerosol material. The theory of the method is developed in detail and is applied successfully to find the optical constants of an o-phosphoric acid aerosol in the 7- to 14-μm infrared. The numerical procedure is shown to introduce an error of less than 1 percent in the determination of the o-phosphoric acid optical constants. Limits on n,k and the particle size distribution for which the method is valid are indicated.

PREFACE

The work described in this report was authorized under Project 1L162662A554, Smoke/Obscurant Technology. This work was started in April 1980 and completed in September 1980.

The use of trade names in this report does not constitute an official endorsement or approval of the use of such commercial hardware or software. This report may not be cited for purposes of advertisement.

Acknowledgments

The authors express their appreciation to Professor Marvin Querry of the University of Missouri-Kansas City for a critical reading of the manuscript.

CONTENTS

DETERMINATION OF OPTICAL CONSTANTS FROM EXTINCTION MEASUREMENTS

1. INTRODUCTION

The interaction of electromagnetic radiation with spherical particles is described by the well-known Lorenz-Mie formalism.[1-3] The optical properties of the particulate material enter into this formalism by way of the optical constants (n, k) which are, respectively, the real and imaginary components of the spectral complex refractive index.

$$\tilde{N}(\lambda) = n(\lambda) - ik(\lambda) \tag{1}$$

where λ denotes the wavelength. With the advent of modern high-speed computers and the development of reliable Mie scattering codes,[4-6] it has become a commonplace numerical procedure to predict the extinction produced by an ensemble of spherical aerosol particles[7-11] once the optical constants (n,k) and the particle size distribution are known. The inverse problem of determining the optical constants from the Lorenz-Mie formalism when measured values of the spectral extinction and the particle size distribution are known has proved to be quite intractable; this is the problem which this paper addresses.

As noted by several workers,[12-14] the experimental difficulties associated with determining the optical constants by transmission, absorption, and reflectance measurements performed on small samples of the aerosol material lead to highly questionable results. A few techniques which avoid these difficulties by using the Lorenz-Mie equations to invert measurements of particulate optical properties to find the optical constants have been reported. Wyatt[15] and Pluchino *et al.*[16] have measured the angularly dependent intensity of laser light scattered from single particles which were suspended in a Millikan oil drop apparatus; the Lorenz-Mie equations were then used to fit the angular scattering data by curve-fitting techniques in which (n,k) appear as parameters.

Another approach is to use extinction measurements which are experimentally simpler than angular scattering measurements, but they have the disadvantage that the Lorenz-Mie inversions are not unique with respect to (n,k) as they are with the angular scattering measurements.[15] Janzen[14] has described a technique for determining the optical constants of a carbon black-water colloid by using the Mie equations to obtain a least squares fit to measured extinction spectra. Janzen's technique overcomes many of the difficulties of the traditional methods, but there are three limitations to his approach: (1) the polydispersity of the particulate material is not accounted for, (2) the optical dispersion of the material is not taken into account, and (3) the optical constants which are found by this technique satisfy the Mie equations, but they are not necessarily the unique (n,k) pair which characterizes the optical behavior of the material. In this paper, we will describe a method of deriving the optical constants of an aerosolized material from extinction measurements; this method overcomes the limitations cited above.

The extinction coefficient (m^2/gm) of an aerosol at wavelength, λ, is defined as

$$\alpha = \frac{\sum_i s_i}{\sum_i m_i} \tag{2}$$

where

s_i = optical cross section of the ith particle (m^2)
m_i = the mass of the ith particle (gm)

and the sum extends over the ensemble of particles contained in the optical path. For a continuous distribution of particles, the expression for the extinction coefficient becomes

$$\alpha = \int \alpha(z) dM \tag{3}$$

where

$\alpha(z)$ = extinction coefficient for a particle of size z
dM = the mass distribution function of the particles

In order to apply the Lorenz-Mie formalism, each aerosol particle will be considered to be spherical with an extinction coefficient which is given by

$$\alpha_o = \frac{3Q_e[\tilde{N}(\lambda), X]}{2\rho D} \tag{4}$$

where

Q_e = the efficiency factor for extinction
X = $\pi D/\lambda$, the size parameter
ρ = the particle density (gm/cm^3)
D = the particle diameter (μm)

It is also convenient to define the dimensionless extinction coefficient

$$\alpha_D = \alpha \bullet \lambda \bullet \rho \tag{5}$$

The difficulties of using extinction measurements to determine the optical constants are illustrated in figure A-1.* For a given wavelength, a value of α_D may correspond to any (n,k) pair lying on the pertinent α_D isopleth; similarly, for a given particle size distribution, the (n,k) pair corresponding to a particular value of α_D is not unique. However, over a wavelength spectrum, the values of $[n(\lambda), k(\lambda)]$ are subject to the constraint imposed by the Kramers-Kronig (KK) dispersion relation.[17-18] In the development which follows, an iterative procedure will be described which, after an initial estimate of $n(\lambda)$ over the wavelength spectrum, employs a simple numerical algorithm to fit the $k(\lambda)$ spectrum to the measured extinction spectrum and the KK dispersion to establish a new estimate of the $n(\lambda)$ spectrum. It will be shown that this procedure will correctly determine the optical constants of the airborne material.

2. THEORY

2.1 Computation of $n(\lambda_o)$.

The Kramers-Kronig relationship between $n(\lambda_o)$ and the $k(\lambda)$ spectrum is given by:

$$n(\lambda_o) = 1 + \frac{2\lambda_o^2}{\pi} P \int_o^\infty \frac{k(\lambda)d\lambda}{\lambda\left(\lambda_o^2 - \lambda\right)^2} \tag{6}$$

where P indicates that the Cauchy principal value is to be taken. The integral in equation 6 is to be evaluated over the entire electromagnetic spectrum; and, since $k(\lambda)$ is known only over a finite region ($\lambda_{min} \leq \lambda \leq \lambda_{max}$) of the spectrum, it is necessary to extend the k-spectrum beyond the wavelength region where data are known experimentally.

The inaccuracies introduced by extending the k-spectrum can be reduced to relative insignificance by employing a subtractive Kramers-Kronig analysis (SKK). Assume that the real part of the refractive index, $n(\lambda_1)$, is known at some wavelength, λ_1, and subtract the KK expression for $n(\lambda_1)$ from the KK expression for $n(\lambda_o)$ in order to obtain the subtractive Kramers-Kronig relationship:[19-21]

$$n(\lambda_o) = n(\lambda_1) + \frac{2\left(\lambda_1^2 - \lambda_o^2\right)}{\pi} P \int_o^\infty \frac{\lambda k(\lambda)d\lambda}{\left(\lambda_o^2 - \lambda^2\right)\left(\lambda_1^2 - \lambda^2\right)} \tag{7}$$

The integral is now evaluated by letting $k(\lambda) = k(\lambda_{min})$ for $0 \leq \lambda \leq \lambda_{min}$ and $k(\lambda) = k(\lambda_{max})$ for $\lambda_{max} \leq \lambda \leq \infty$. In general, these are not good physical approximations

* All figures are in the appendix.

for $k(\lambda)$ in the spectral regions where $k(\lambda)$ has not been measured; but, as mentioned previously, this approximation will have an insignificant effect on the result produced by the SKK algorithm.

2.2 Calculation of $k(\lambda)$.

In the previous section, it was shown that SKK analysis can be used to calculate $n(\lambda_o)$ once $n(\lambda_1)$ and $k(\lambda)$ are known. A method of obtaining $k(\lambda)$ from measurements of the extinction spectrum, $\alpha(\lambda)$, and the particle size distribution will now be developed. For a continuous distribution of spherical particles, the expression for the extinction coefficient of a single spherical particle with diameter, D, (equation 4) may be integrated to find an expression for the extinction coefficient of the particle ensemble at wavelength λ:

$$\alpha(n,k) = \int \alpha_o(n,k,D)\, dM \tag{8}$$

For this study the mass size distribution was described by the log-normal distribution function

$$dM = \frac{1}{\sqrt{2\pi}} \frac{1}{\ell n\sigma_g} e^{-1/2\left[\ell n(D/Dm)/\ell n\sigma_g\right]^2} d\ell nD \tag{9}$$

where

D_m = mass median diameter (MMD)
σ_g = geometric standard deviation

It will now be assumed that an estimate of $n(\lambda) = n_o$ is available from the SKK analysis; and, therefore, the extinction coefficient depends on k only

$$\alpha(k) = \alpha(n_o,k) \tag{10}$$

The isopleths of α_D, shown in figure A-1, depict the behavior of the integral kernel, α_o, in the expression for $\alpha(n,k)$ as the size parameter varies. Many of the interesting features of these isopleths are due to optical resonance phenomena.[10] The resonance due to the first surface polariton mode for $X \to 0$ is located at the point $\xi_o = (0, \sqrt{2})$ and moves according to the equation[22]

$$k \approx \sqrt{2}\left(1 + 6/5\ X^2\right)^{1/2} \tag{11}$$

to larger values of k as the size parameter increases. Also, the resonances due to the bulk polariton modes can be seen to move along the n axis toward the k axis as the size parameter increases (figure A-1, E to I).

Let us now divide the n,k plane by a horizontal line through the locus ξ_o and accept values of k which lie in the lower half of the divided n,k plane; i.e., $0 \leq k \leq \sqrt{2}$. In this region, the extinction coefficient is a single-valued function in the vicinity of the first surface polariton resonance and no significant loss of generality is incurred by imposing this condition since most condensed matter has k values which lie in this region. If $n(\lambda)$ is now considered to be fixed at some value n_o, it can be seen in figure A-1 that, in general, the dimensionless extinction coefficient increases monotonically with respect to k; this fact forms the basis of the procedure for computing $k(\lambda)$. Since the isopleths of α_D represent the integral kernel of equation 10, $\alpha(k)$ itself is expected to be monotonic with respect to k over a wider range of n than is indicated in figure A-1. This has been previously demonstrated in work by Jennings *et al.*[11] who computed isopleths in n,k space of the extinction coefficient at 10.6 μm for log-normally distributed aerosols which had number median diameters, D_n, of 2.0 and 20.0 μm and $\sigma_g = 1.5$. For these cases, $\alpha(k)$ is shown to be monotonic for $10^{-3} \leq k \leq \sqrt{2}$, when $0.1 \leq n \leq 8$ for $D_n = 2.0$ μm and when $0.1 \leq n \leq 4$ for $D_n = 20.0$ μm.

The effects on the monotonicity of the extinction coefficient which result from changing the particle size distribution and the real part of the complex refractive index are shown in the curves of figure A-2. In these curves, the dimensionless extinction coefficient, integrated over the indicated log-normal size distribution functions, is plotted with n fixed as a function of the mass median size parameter

$$X_m = \pi D_m/\lambda \tag{12}$$

for values of k between 0 and $\sqrt{2}$. The range in X_m over which α_o remains monotonic is determined by the interaction between the resonances due to the bulk polaritons and the tendency of the polydispersity to smooth out such resonance effects. Also, since a nonzero imaginary part of the refractive index acts to damp out the resonances, the extinction curves for $\alpha_o(0)$ display the most abundant resonant structure. For small values of X_m, $\alpha_D(k)$ increases monotonically with respect to k; this monotonic behavior of $\alpha_D(k)$ continues as X_m increases until the $\alpha_D(0)$ curve crosses the nearest neighboring $\alpha_D(k)$ curve. The value of X_m at this crossing point defines an upper limit, $X_{m\ell}$, below which $\alpha_D(k)$ is monotonically increasing with respect to k. The value of $X_{m\ell}$ depends both on the polydispersity of the aerosol and on the value of the real part of the complex refractive index. The table shows the approximate values of $X_{m\ell}$ for the curves of figure A-2. Once X_m becomes larger than $X_{m\ell}$, the behavior of $\alpha_D(k)$ is not generally predictable since it depends in large measure on the resonant structure of the $\alpha_D(0)$ curve. For X_m larger than $X_{m\ell}$, it does not appear possible to determine k uniquely from extinction data. Figure A-3 shows explicitly the variation of the dimensionless extinction coefficient with k as X_m increases for the case in which $n = 2$ and $\sigma_g = 1.4$. The curves for $X_m = 1.38$ and $X_m = 1.44$ bracket $X_{m\ell}$ for this case (see the table).

Table. Approximate Values of the Upper Monotonicity Limit for the Mass Median Size Parameter

σ_g	n		
	1.33	2.0	3.0
1.1	3.55	1.35	0.89
1.4	3.55	1.41	0.81
2.0	4.68	1.78	0.89
3.0	9.77	3.39	1.23

From the discussion above, it may be concluded that the extinction coefficient will be monotonic with respect to k for the range of optical constants and particle sizes likely to be encountered in many practical problems in aerosol physics. As shown in figure A-4, it now becomes, in principle, a simple matter to determine k numerically. α_c is the extinction coefficient computed from equation 10 using the current estimate for k and the experimentally determined size distribution; α_e is the measured value of the extinction coefficient. Successive estimates of k are made until $|\alpha_c - \alpha_e| < \delta$, where δ is determined by the precision to which the extinction coefficient can be measured.

2.3 Algorithm for computing optical constants.

The procedures developed above may be combined into an algorithm for computing the optical constants as shown in the flow chart of figure A-5. The computation is started by taking $n(\lambda)$ equal to a constant which we usually choose to be 1.3. Successive calculations of $k(\lambda)$ and $n(\lambda)$ are then made until convergence is obtained. The algorithm was implemented by means of a FORTRAN program written for use on a Univac 1108 computer. All Mie calculations were carried out by means of a modified version of Dave's DBMIE subroutine,[4] and the original version of the SKK routine used in this study was developed by Querry.*

3. EXPERIMENTAL PROCEDURE AND RESULTS

An extinction spectrum and particle size distribution for o-phosphoric acid were measured in order to confirm the theory developed in section 2. Figure A-6 shows a diagram of the experimental arrangement employed for these measurements. The o-phosphoric acid was disseminated in a 22-m^3 test chamber by spraying the acid solution through a pneumatic nozzle; the acid aerosol was stirred continuously throughout the experiment in order to maintain a uniform aerosol concentration. An Exotech model 10-24 radiometer with a circular variable filter monochrometer was used to scan the 7- to 14-μm infrared region at a rate of 15 scans per minute; the path length through the aerosol was 3.05 m. The radiometer data were recorded on analog tape with a Hewlett-Packard model 3960 recorder. Particle

* Querry, M. R. Private communication. 1967.

size samples were taken with an Andersen model 2000 cascade impactor, and the aerosol mass concentration was determined from samples taken on glass fiber filters.

A Quad Systems model 721 digitizer was used to convert the analog radiometer data to digital form, and the digitized data were written on a magnetic tape for use in subsequent computer processing. The extinction spectrum was determined from the digitized data by Beer's law

$$\alpha_e = \frac{-1}{CL} \ln T \tag{13}$$

where

C = aerosol mass concentration (gm/m^3)
L = optical path length (m)
T = transmittance

The measured acid concentration of the aerosol droplets was approximately 65% by weight and the log-normal particle size distribution as estimated from the cascade impactor results had the parameters $D_m = 3.3$ μm and $\sigma_g = 2.0$. Figure A-7 compares the experimentally determined extinction spectrum with a spectrum computed using the optical constant data[23] for 65% by weight of o-phosphoric acid. The experimental spectrum was produced by averaging 45 radiometer scans; and figure A-8 shows a plot of the percent difference between the computed and experimental spectra as a function of wavelength.

4. OPTICAL CONSTANT RESULTS

The experimental data for o-phosphoric acid were analyzed according to the procedure described in figure A-5; the known value of $n(\lambda)$ was taken to be 1.604 at 10.0 μm.[23] After four iterations, the calculations converged to produce the solution shown in figure A-9 for $n(\lambda)$ and in figure A-10 for $k(\lambda)$. For purposes of comparison, $n(\lambda)$ and $k(\lambda)$ for 65% o-phosphoric acid are also plotted in figures A-9 and A-10; figures A-11 and A-12 are plots of the percent difference between the computed values of the optical constants and the measured values for 65% o-phosphoric acid. Notice that the spectral structure of the percent difference for $\alpha(\lambda)$ (figure A-8) is very similar to the spectral structure of the percent difference for $k(\lambda)$ (figure A-12). This suggests that differences between the computed and measured values of the optical constants are due to experimental error in measuring the extinction spectrum and particle size distribution. In order to determine the amount of error introduced by the computational procedure, the computed spectrum from figure A-7 was used as the input extinction spectrum from which the optical constants were to be computed. The computation converged after five iterations, and the results for the optical constants are compared with the measured 65% o-phosphoric acid data in figures A-13 and A-14. The average percent difference between the computed and the measured results for (n,k) was less than 1 percent over the 7- to 14-μm spectral region. Therefore, it was concluded that the dominant contribution to the difference between the optical constants computed from

the o-phosphoric acid extinction data and the measured values was due to error in measuring the extinction spectrum and the particle size distribution of the aerosol.

5. CONCLUSION

We have described an entirely new approach to the determination of the optical constants of particulate materials. This new method avoids the experimental difficulties and errors associated with the traditional methods of finding the optical constants of aerosol materials. It is an iterative procedure which, after an initial estimate of $n(\lambda)$ over the wavelength spectrum, employs a simple numerical algorithm to fit the $k(\lambda)$ spectrum to a measured extinction spectrum and the KK dispersion to establish a new estimate of the $n(\lambda)$ spectrum. The values of $k(\lambda)$ are restricted to the range 0 to $\sqrt{2}$, and the numerical algorithm for finding $k(\lambda)$ is valid for a wide range of $n(\lambda)$ and particle size distributions as shown in the table. The value of $n(\lambda)$ must be known for one wavelength in the spectral region being investigated.

The theory of the method was developed in detail and was successfully applied to the determination of the optical constants of an o-phosphoric acid aerosol in the 7- to 14-μm infrared. The numerical procedure was shown to introduce an error of less than 1 percent in the determination of the o-phosphoric acid optical constants.

LITERATURE CITED

1. Van de Hulst, H. C. Light Scattering by Small Particles. Wiley, New York, New York. 1957.

2. Deirmendjian, D. Electromagnetic Scattering on Spherical Polydispersions. Elsevier, New York, New York. 1969.

3. Kerker, M. The Scattering of Light and Other Electromagnetic Radiation. Academic Press, New York, New York. 1969.

4. Dave, J. V. Report No. 320-3237. IBM Scientific Center, Palo Alto, California. 1968.

5. Grehan, G., and Gouesbet, G. Appl. Opt. 18, 3489 (1979).

6. Wiscombe, W. J. Ibid. 19, 1505 (1980).

7. Wells, W. C., Gal, G., and Munn, M. W. Ibid. 16, 654 (1977).

8. Patterson, E. M. Ibid. 16, 2414 (1977).

9. Jennings, S. G., Pinnick, R. G., and Auvermann, H. J. Ibid. 17, 3922 (1978).

10. Roessler, D. M., and Faxvog, F. R. Ibid. 18, 1399 (1979).

11. Jennings, S. G., Pinnick, R. G., and Gillespie, J. B. Ibid. 18, 1368 (1979).

12. Bergstrom, R. W. Beitr. Phys. Atmos. 46, 198 (1973).

13. Toon, O. B., Pollack, J. B., and Khare, B. N. J. Geophys. Res. 81, 5733 (1976).

14. Janzen, J. J. Colloid Interface Sci. 69, 436 (1979).

15. Wyatt, P. J. Appl. Opt. 19, 975 (1980).

16. Pluchino, A. B., Goldberg, S. S., Dowling, J. M., and Randall, C. M. Ibid. 19, 3370 (1980).

17. Cardona, M. Optical Properties of Solids. S. Nudelman and S. S. Mitra, editors. Plenum Press, New York, New York. 1969.

18. Landau, L. D., and Lifshitz, E. M. Electrodynamics of Continuous Media. Pergamon Press, Oxford, England. 1960.

19. Bachrach, R. Z., and Brown, F. C. Phys. Rev. B1, 818 (1970).

20. Ahrenkiel, R. K. J. Opt. Soc. Am. 61, 1651 (1971).

21. Hale, G. M., and Querry, M. R. Appl. Opt. 12, 555 (1973).

22. Gilra, D. P. Collective Excitations in Small Solid Particles and Astronomical Applications. Ph.D. Thesis. 1972.

23. Querry, M. R. Molecular and Crystalline Electromagnetic Properties of Selected Condensed Materials in the Infrared. Final Report. DAAG-29-76-GS-0185. US Army Research Office, Research Triangle Park, North Carolina 27709. 1979.

APPENDIX

FIGURES

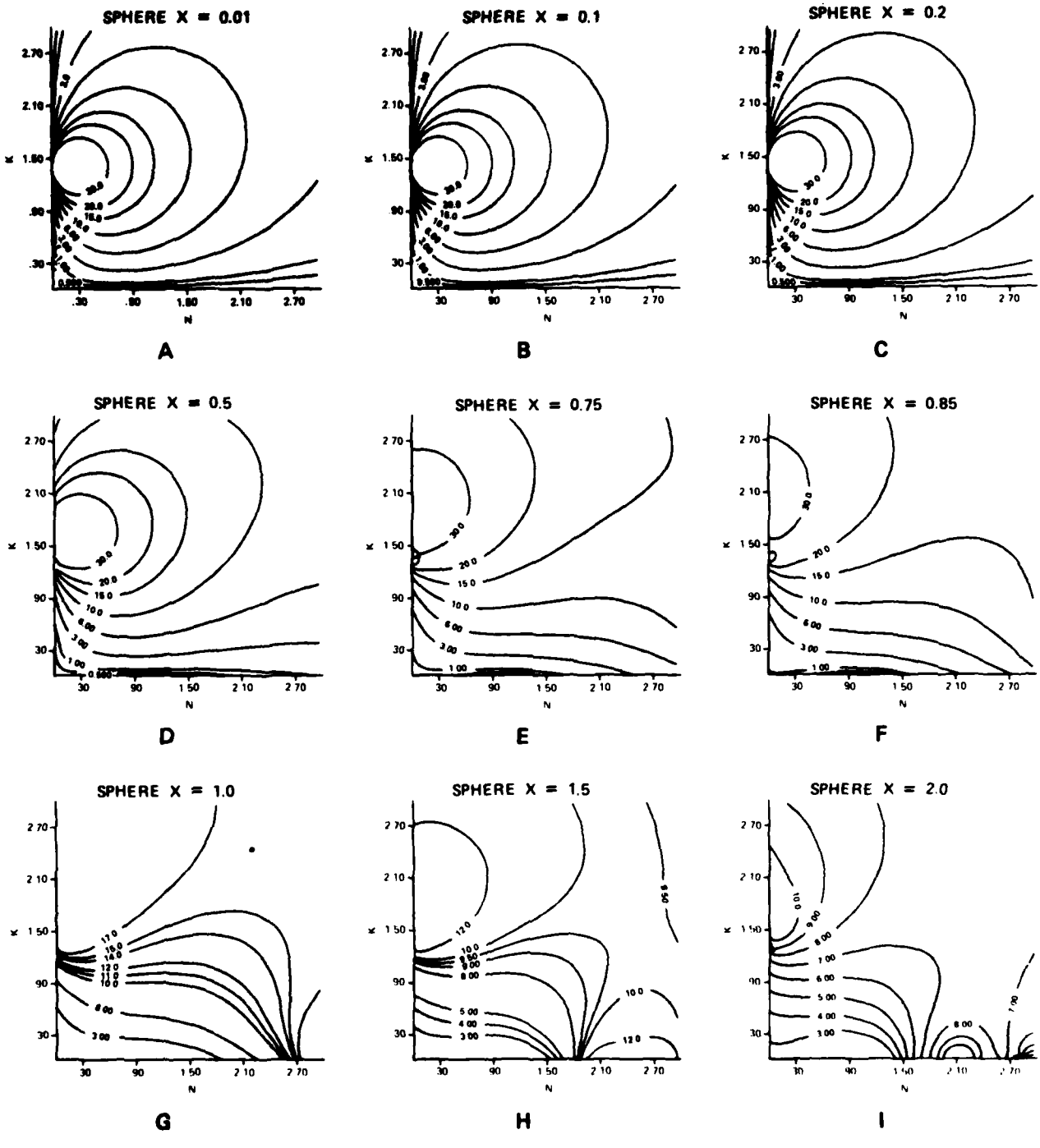

Figure A-1. Isopleths in n,k Space of the Dimensionless Extinction Coefficient for Spheres with the Indicated Size Parameters

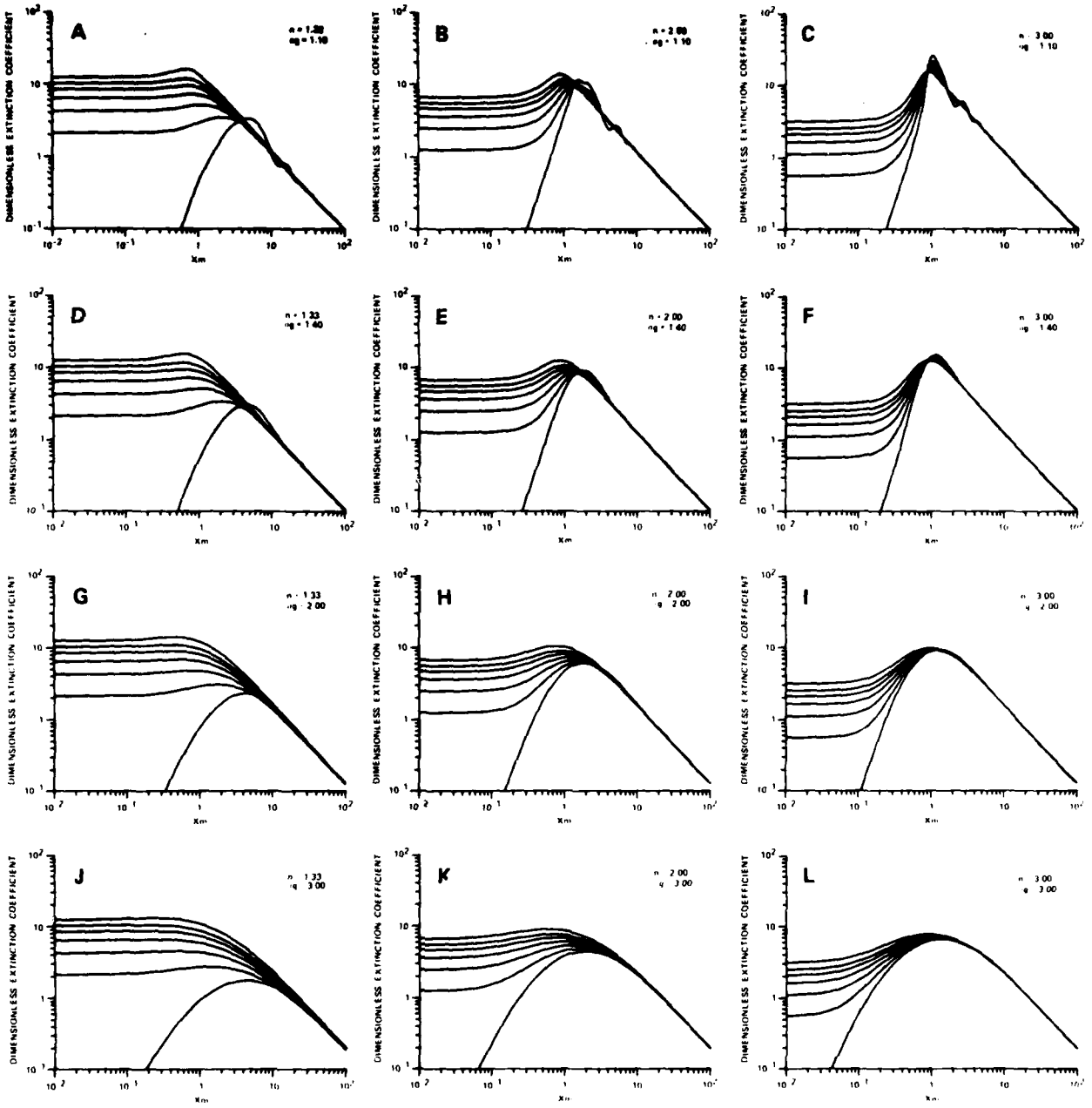

Figure A-2. Dimensionless Extinction Coefficient, α_D, for Log-Normally Distributed Spheres as a Function of Mass Median Size Parameter, X_m

Individual curves are for k = 0, 0.2, 0.4, 0.6, 0.8, 1.0, 2 and are easily identified, since α_D is monotonically increasing with respect to k at the left-hand side of the plots.

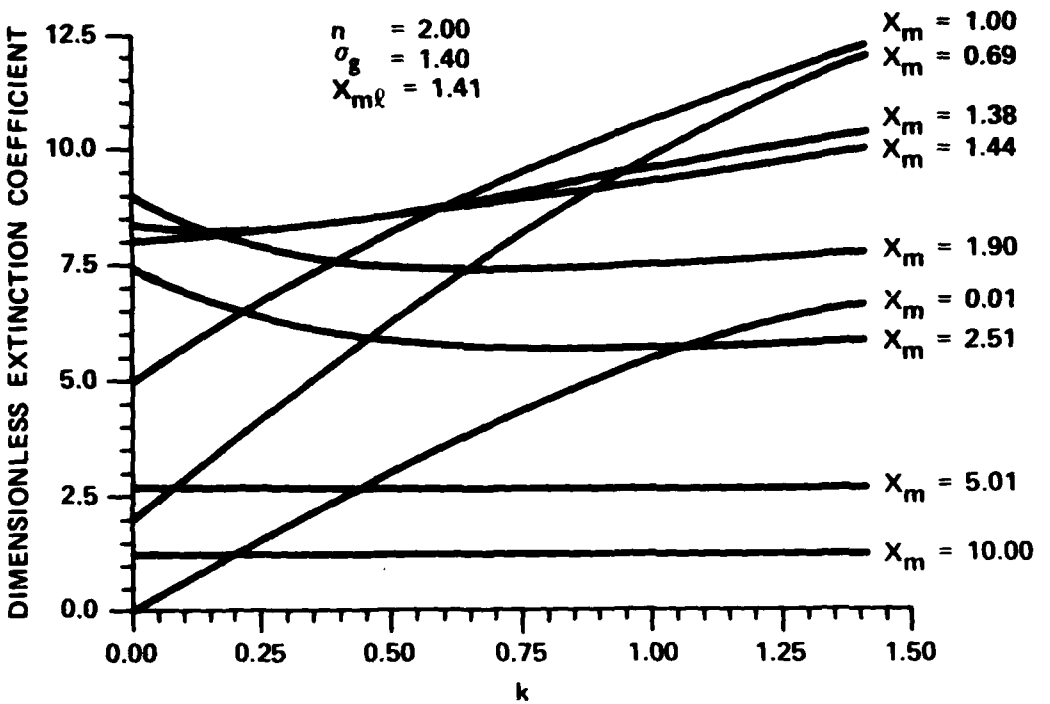

Figure A-3. Variation of the Dimensionless Extinction Coefficient with k as X_m Increases
The curves for X_m = 1.38 and X_m = 1.44 bracket $X_{m\ell}$.

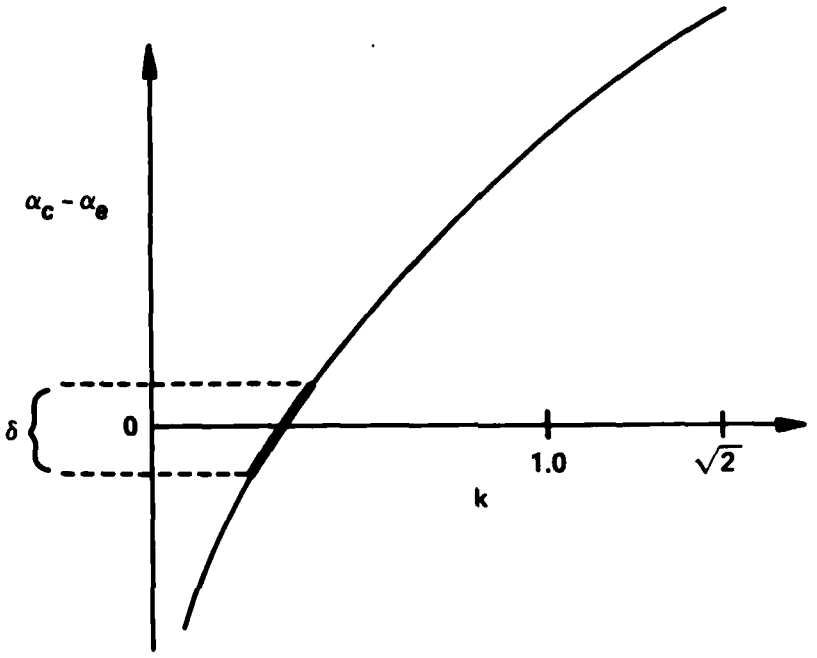

Figure A-4. Illustration of the Numerical Procedure for Calculating k

α_e is the measured extinction coefficient and α_c is the computed extinction coefficient.

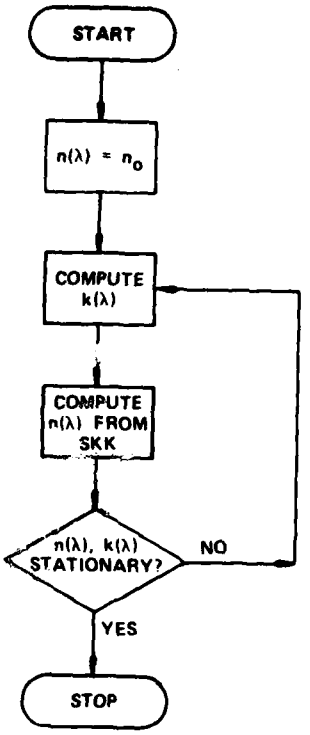

Figure A-5. Flowchart of the Algorithm for Determining the Optical Constants n,k from Extinction Measurements

n_o is an initial, assumed value of the real part of the refractive index. n_o is typically taken to be 1.3.

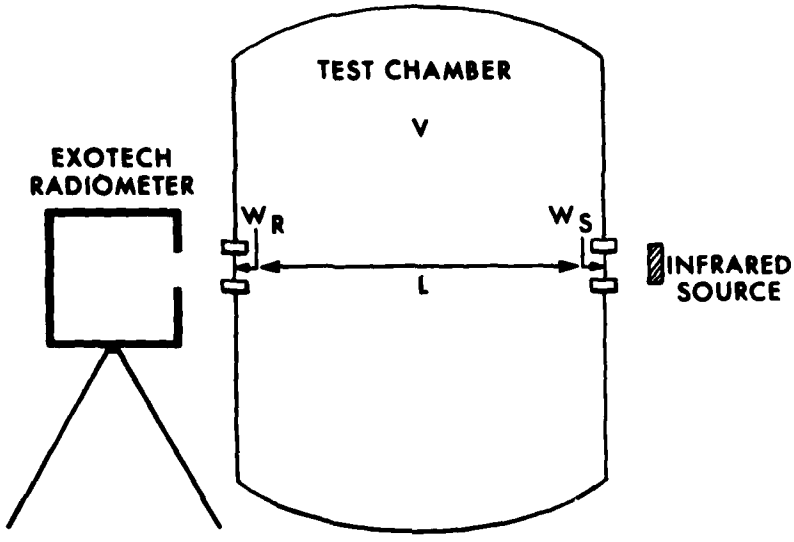

W_R = Radiometer Window - Polyethylene

W_S = Source Window - Polyethylene

L = Path Length, 3.05 m

V = Chamber Volume, 22 m^3

Figure A-6. Experimental Arrangement Used for o-Phosphoric Acid Aerosol Measurement

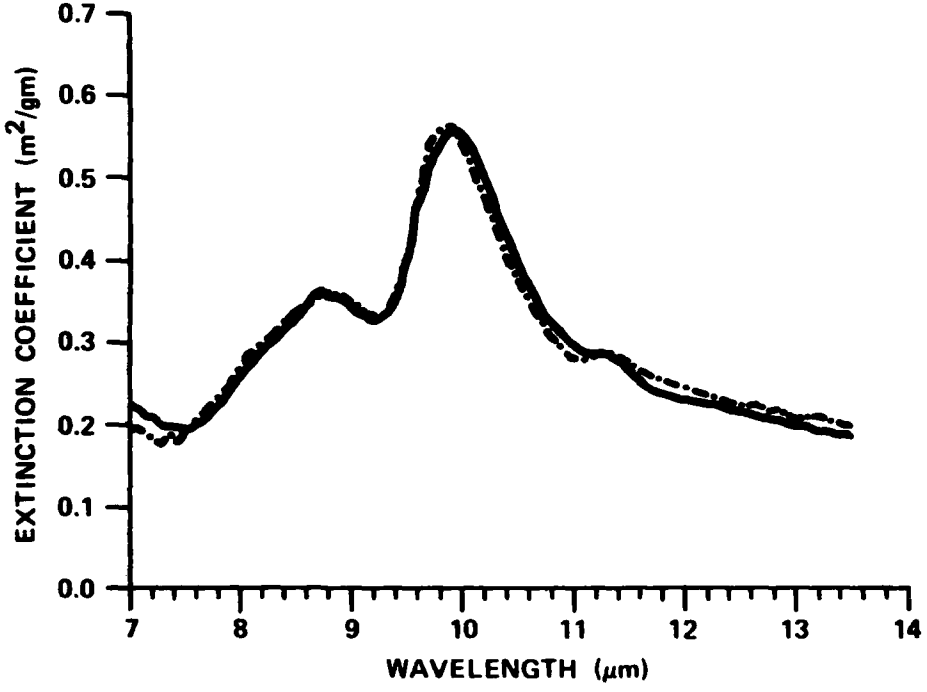

Figure A-7. Comparison of the Experimentally Determined Extinction Spectrum (Dashed Line) with a Computed Extinction Spectrum (Solid Line) for 65% o-Phosphoric Acid

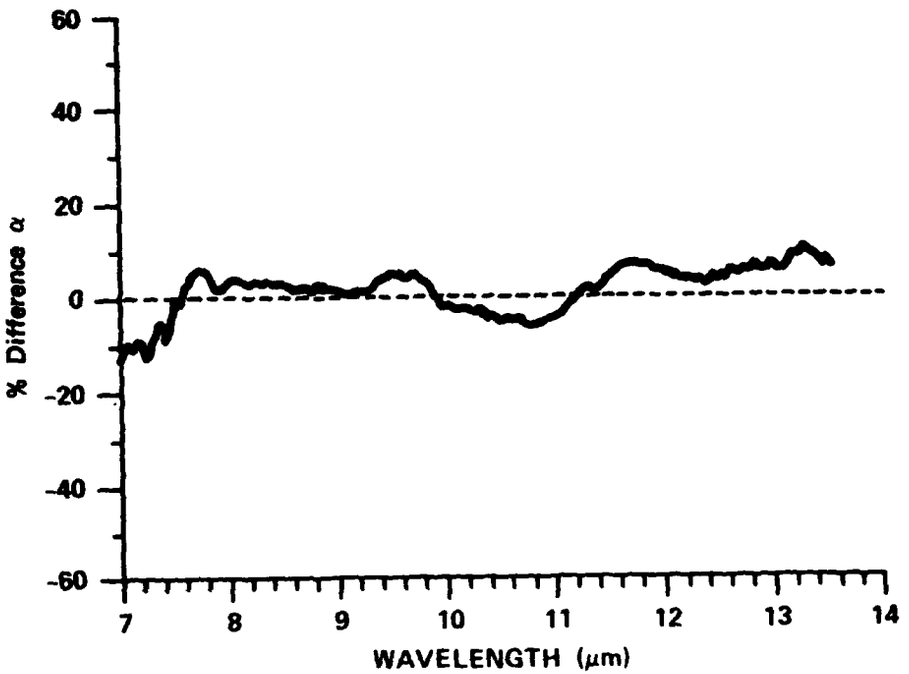

Figure A-8. Percent Difference between the Computed and Measured Extinction Spectrum as a Function of Wavelength

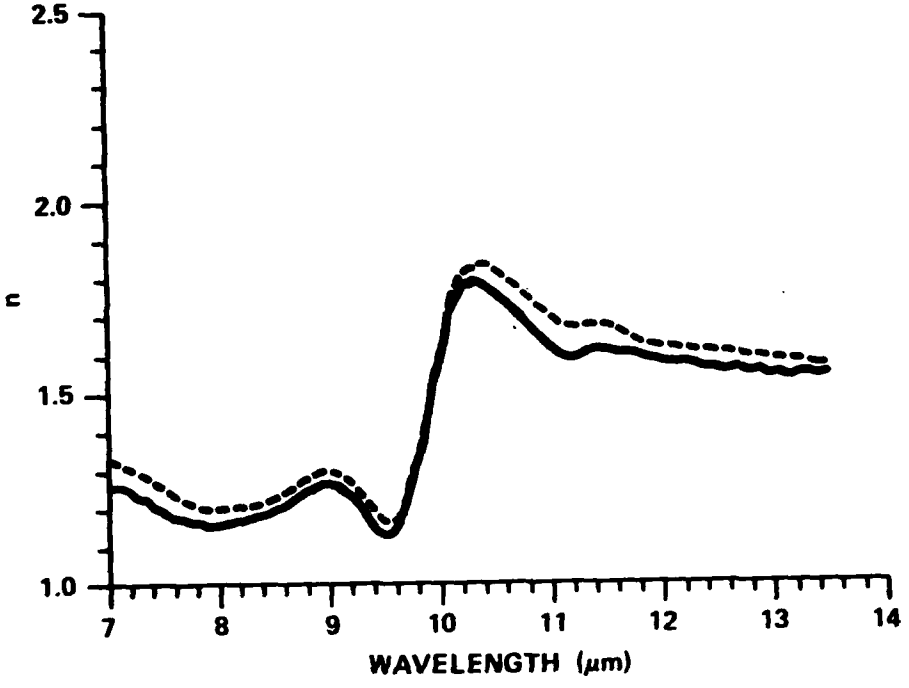

Figure A-9. Comparison of n(λ) Determined from Extinction Measurements (Solid Curve) with the Measured Values for 65% o-Phosphoric Acid (Dashed Curve)

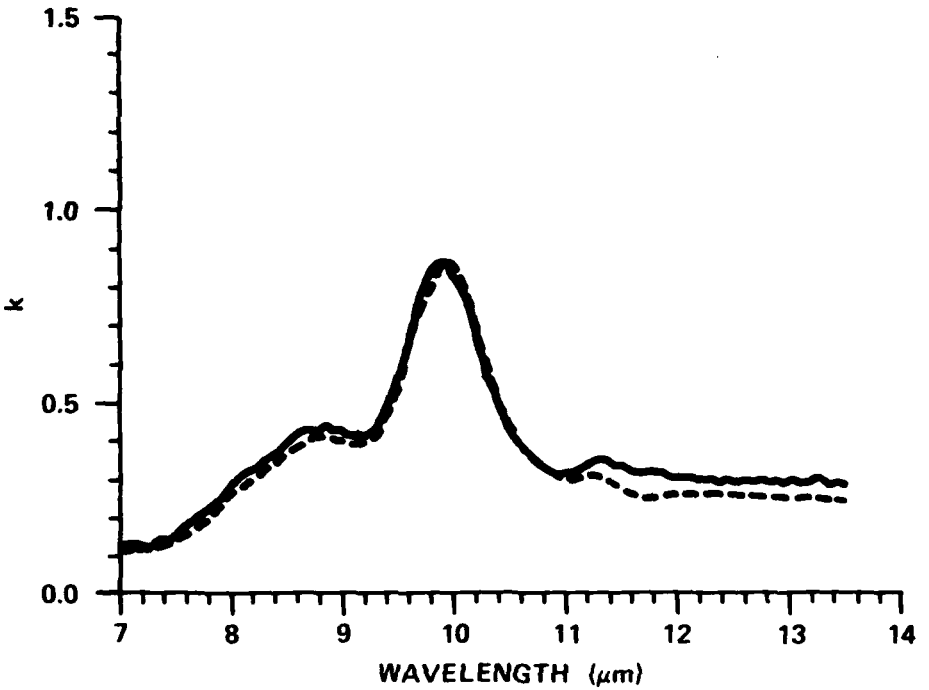

Figure A-10. Comparison of k(λ) Determined from Extinction Measurements (Solid Curve) with the Measured Values for 65% o-Phosphoric Acid (Dashed Curve)

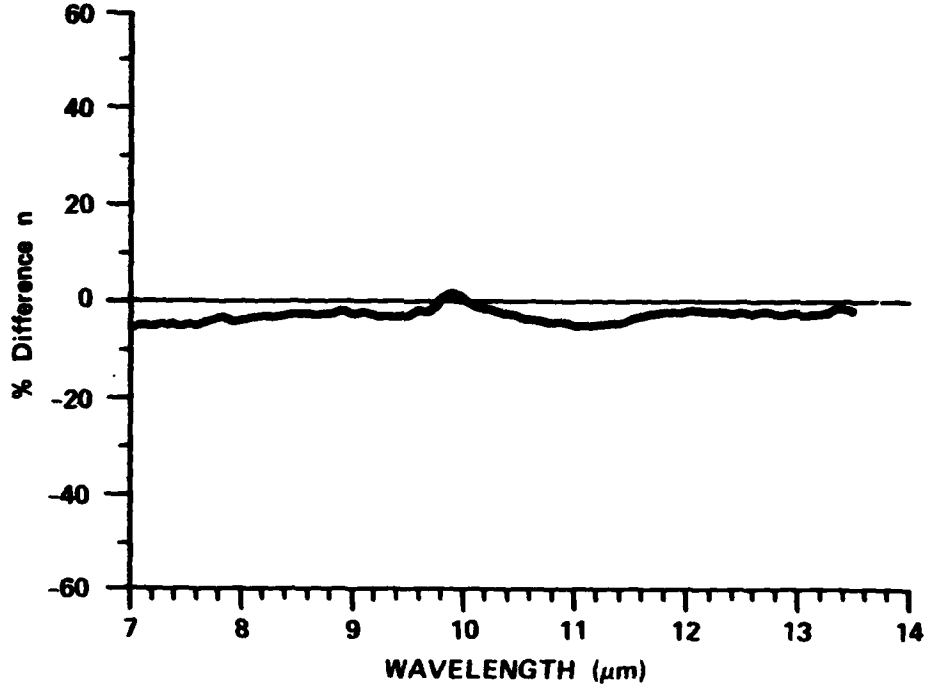

Figure A-11. Percent Difference between n(λ) Determined from Extinction Measurements and the Values of n(λ) for 65% o-Phosphoric Acid

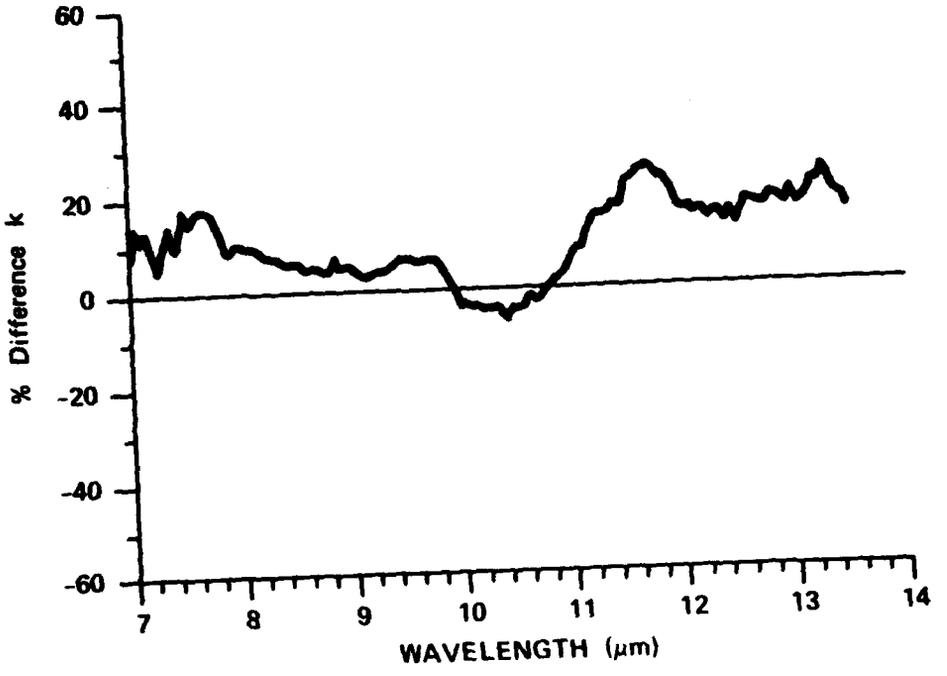

Figure A-12. Percent Difference between k(λ) Determined from Extinction Measurements and the Values of k(λ) for 65% o-Phosphoric Acid

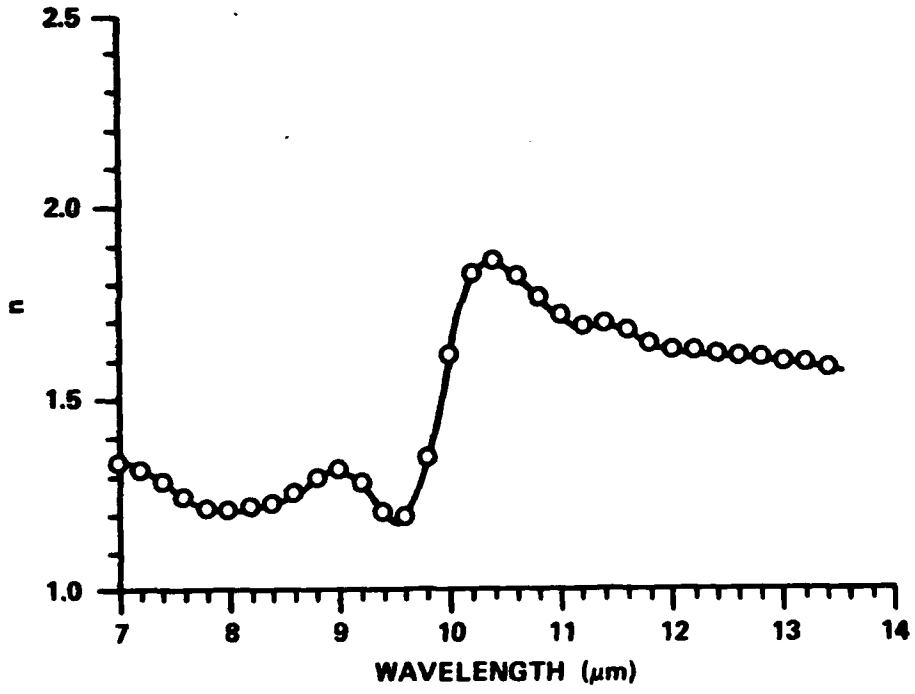

Figure A-13. Comparison of n(λ) Derived from a Spectrum (Circles) Computed from Lorenz-Mie Theory with the Real Parts Used in the Computation (Solid Curve)

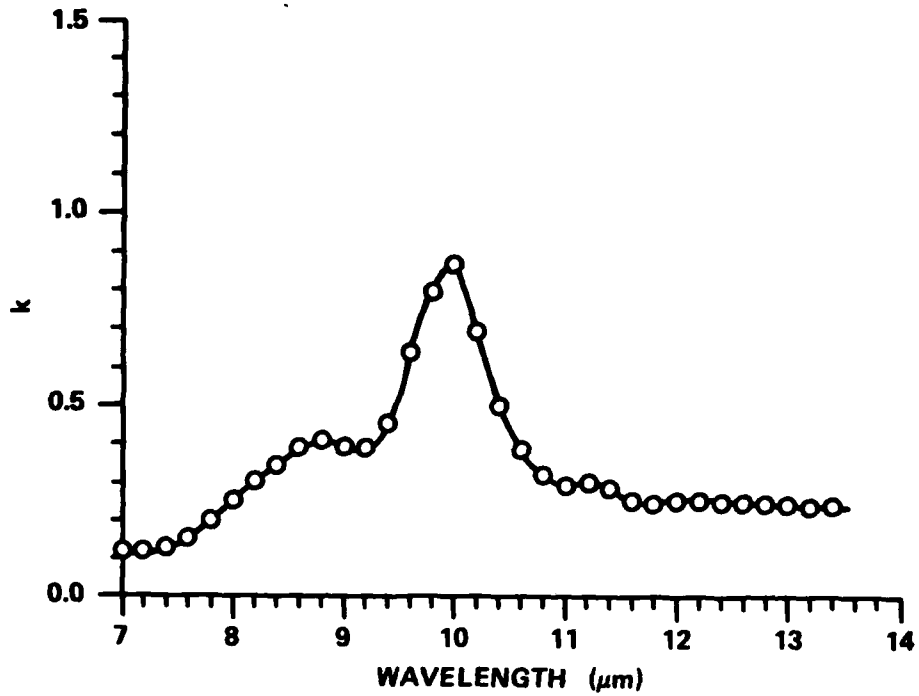

Figure A-14. Comparison of k(λ) Derived from a Spectrum (Circles) Computed from Lorenz-Mie Theory with the Imaginary Parts Used in the Computation (Solid Curve)

DISTRIBUTION LIST 5

Names	Copies
CHEMICAL SYSTEMS LABORATORY	
ATTN: DRDAR-CLF	1
ATTN: DRDAR-CLJ-R	3
ATTN: DRDAR-CLJ-L	3
ATTN: DRDAR-CLJ-M	1
ATTN: DRDAR-CLJ-P	1
ATTN: DRDAR-CLT-E	1
ATTN: DRDAR-CLN	2
ATTN: DRDAR-CLW-C	1
ATTN: DRDAR-CLB-C	1
ATTN: DRDAR-CLB-P	1
ATTN: DRDAR-CLB-PA	1
ATTN: DRDAR-CLB-R	1
ATTN: DRDAR-CLB-T	1
ATTN: DRDAR-CLB-TE	1
ATTN: DRDAR-CLY-A	1
ATTN: DRDAR-CLY-R	1
ATTN: DRDAR-CLR-I	1
COPIES FOR AUTHOR(S):	
Research Division	4
DEPARTMENT OF DEFENSE	
Defense Technical Information Center ATTN: DTIC-DDA-2 Cameron Station, Building 5 Alexandria, VA 22314	12
Director Defense Intelligence Agency ATTN: DB-4G1 Washington, DC 20301	1
Special Agent in Charge ARO, 902d Military Intelligence GP ATTN: IAGPA-A-AN Aberdeen Proving Ground, MD 21005	1
Commander SED, HQ, INSCOM ATTN: IRFM-SED (Mr. Joubert) Fort Meade, MD 20755	1
DEPARTMENT OF THE ARMY	
HQDA (DAMO-NCC) WASH DC 20310	1
Deputy Chief of Staff for Research, Development & Acquisition ATTN: DAMA-CSS-C	1
ATTN: DAMA-ARZ-D Washington, DC 20310	1
US Army Research and Standardization Group (Europe) ATTN: DRXSN-E-SC Box 65, FPO New York 09510	1
HQDA (DAMI-FIT) WASH, DC 20310	1
Commander DARCOM, STITEUR ATTN: DRXST-STI Box 48, APO New York 09710	1
Commander US Army Science & Technology Center-Far East Office ATTN: MAJ Borges APO San Francisco 96328	1
Commander 2d Infantry Division ATTN: EAIDCOM APO San Francisco 96224	1
Commander 5th Infantry Division (Mech) ATTN: Division Chemical Officer Fort Polk, LA 71459	1
OFFICE OF THE SURGEON GENERAL	
Commander US Army Medical Bioengineering Research and Development Laboratory ATTN: SGRD-UBD-AL Fort Detrick, Bldg 568 Frederick, MD 21701	1
Headquarters US Army Medical Research and Development Command ATTN: SGRD-PL Fort Detrick, MD 21701	1

Commander
USA Biomedical Laboratory
ATTN: SGRD-UV-L 1
Aberdeen Proving Ground, MD 21010

US ARMY HEALTH SERVICE COMMAND

Superintendent
Academy of Health Sciences
US Army
ATTN: HSA-CDH 1
ATTN: HSA-IPM 1
Fort Sam Houston, TX 78234

US ARMY MATERIEL DEVELOPMENT AND READINESS COMMAND

Commander
US Army Materiel Development and Readiness Command
ATTN: DRCLDC 1
ATTN: DRCSF-P 1
5001 Eisenhower Ave
Alexandria, VA 22333

Project Manager Smoke/Obscurants
ATTN: DRCPM-SMK 1
Aberdeen Proving Ground, MD 21005

Commander
US Army Foreign Science & Technology Center
ATTN: DRXST-MT3 1
220 Seventh St., NE
Charlottesville, VA 22901

Director
US Army Materiel Systems Analysis Activity
ATTN: DRXSY-MP 1
ATTN: DRXSY-T (Mr. Metz) 2
Aberdeen Proving Ground, MD 21005

Commander
US Army Missile Command
Redstone Scientific Information Center
ATTN: DRSMI-RPR (Documents) 1
Redstone Arsenal, AL 35809

Director
DARCOM Field Safety Activity
ATTN: DRXOS-C 1
Charlestown, IN 47111

Commander
US Army Natick Research and Development Command
ATTN: DRDNA-VR 1
ATTN: DRDNA-VT 1
Natick, MA 01760

US ARMY ARMAMENT RESEARCH AND DEVELOPMENT COMMAND

Commander
US Army Armament Research and Development Command
ATTN: DRDAR-LCA-L 1
ATTN: DRDAR-LCE 1
ATTN: DRDAR-LCE-C 1
ATTN: DRDAR-LCU 1
ATTN: DRDAR-LCU-CE 1
ATTN: DRDAR-PMA (G.R. Sacco) 1
ATTN: DRDAR-SCA-W 1
ATTN: DRDAR-TSS 2
ATTN: DRCPM-CAWS-AM 1
ATTN: DRCPM-CAWS-SI 1
Dover, NJ 07801

Director
Ballistic Research Laboratory
ARRADCOM
ATTN: DRDAR-TSB-S 1
Aberdeen Proving Ground, MD 21005

US ARMY ARMAMENT MATERIEL READINESS COMMAND

Commander
US Army Armament Materiel Readiness Command
ATTN: DRSAR-ASN 1
ATTN: DRSAR-PDM 1
ATTN: DRSAR-SF 1
Rock Island, IL 61299

Commander
US Army Dugway Proving Ground
ATTN: Technical Library Docu Sect 1
Dugway, UT 84022

US ARMY TRAINING & DOCTRINE COMMAND

Commandant
US Army Infantry School
ATTN: NBC Division 1
Fort Benning, GA 31905

Commandant
USAMP&CS/TC&FM
ATTN: ATZN-CM-CDM 1
Fort McClellan, AL 36205

Commander
US Army Infantry Center
ATTN: ATSH-CD-MS-C 1
Fort Benning, GA 31905

Commander
US Army Infantry Center
Directorate of Plans & Training
ATTN: ATZB-DPT-PO-NBC 1
Fort Benning, GA 31905

Commander
USA Training and Doctrine Command
ATTN: ATCD-Z 1
Fort Monroe, VA 23651

Commander
USA Combined Arms Center and
Fort Leavenworth
ATTN: ATZL-CA-COG 1
ATTN: ATZL-CAM-IM 1
Fort Leavenworth, KS 66027

Commander
US Army TRADOC System
Analysis Activity
ATTN: ATAA-SL 1
White Sands Missile Range, NM 88002

US ARMY TEST & EVALUATION COMMAND

Commander
US Army Test & Evaluation Command
ATTN: DRSTE-CM-F 1
ATTN: DRSTE-CT-T 1
Aberdeen Proving Ground, MD 21005

DEPARTMENT OF THE NAVY

Commander
Naval Explosive Ordnance
Disposal Facility
ATTN: Army Chemical Officer
Code AC-3 1
Indian Head, MD 20640

Commander
Naval Weapons Center
ATTN: Technical Library (Code 343) 1
China Lake, CA 93555

Commander Officer
Naval Weapons Support Center
ATTN: Code 5042 (Dr. B.E. Douda) 1
Crane, IN 47522

US MARINE CORPS

Director, Development Center
Marine Corps Development and
Education Command
ATTN: Fire Power Division 1
Quantico, VA 22134

DEPARTMENT OF THE AIR FORCE

HQ Foreign Technology Division (AFSC)
ATTN: TQTR 1
Wright-Patterson AFB, OH 45433

HQ AFLC/LOWMM 1
Wright-Patterson AFB, OH 45433

OUTSIDE AGENCIES

Battelle, Columbus Laboratories
ATTN: TACTEC 1
505 King Avenue
Columbus, OH 43201

Toxicology Information Center,
WG 1008
National Research Council 1
2101 Constitution Ave., NW
Washington, DC 20418

ADDITIONAL ADDRESSEE

Commander
US Army Environmental Hygiene Agency
ATTN: Librarian, Bldg 2100 1
Aberdeen Proving Ground, MD 21010

Stimson Library (Documents) 1
Academy of Health Sciences
Bldg. 2840
Fort Sam Houston, TX 78234

Figure A-3. Variat

Figure A-4. Illustration of the numerical procedure for c

α_e is the measured extinction coefficient and α_c
extinction coefficient.